

Interplay between Distributed AI Workflow and URLLC

Milad Ganjalizadeh^{*†}, Hossein S. Ghadikolaei^{*}, Johan Haraldson^{*}, and Marina Petrova^{†‡}

^{*}Ericsson Research, Sweden

[†]School of Electrical Engineering and Computer Science, KTH Royal Institute of Technology, Stockholm, Sweden

[‡]Mobile Communications and Computing, RWTH Aachen University, Germany

Email: {milad.ganjalizadeh, hossein.shokri,ghadikolaei, johan.haraldson}@ericsson.com, petrovam@kth.se

Abstract—Distributed artificial intelligence (AI) has recently accomplished tremendous breakthroughs in various communication services, ranging from fault-tolerant factory automation to smart cities. When distributed learning is run over a set of wireless connected devices, random channel fluctuations, and the incumbent services simultaneously running on the same network affect the performance of distributed learning. In this paper, we investigate the interplay between distributed AI workflow and ultra-reliable low latency communication (URLLC) services running concurrently over a network. Using 3GPP compliant simulations in a factory automation use case, we show the impact of various distributed AI settings (e.g., model size and the number of participating devices) on the convergence time of distributed AI and the application layer performance of URLLC. Unless we leverage the existing 5G-NR quality of service handling mechanisms to separate the traffic from the two services, our simulation results show that the impact of distributed AI on the availability of the URLLC devices is significant. Moreover, with proper setting of distributed AI (e.g., proper user selection), we can substantially reduce network resource utilization, leading to lower latency for distributed AI and higher availability for the URLLC users. Our results provide important insights for future 6G and AI standardization.

Index Terms—6G, availability, distributed AI, factory automation, federated learning, quality-of-service, URLLC.

I. INTRODUCTION

Future 6G networks are envisioned as an unprecedented evolution from connected things to connected intelligence, thereby serving as the backbone of a cyber-physical world with the integration of connected devices, intelligence, and humans [1]. Numerous 6G artificial intelligence (AI) applications have emerged recently to improve efficiency and system performance in many vertical sectors, such as industrial automation [2], autonomous driving [3], and enhanced mobile broadband [4]. Centralized training of the models can be impractical in many wireless communication applications because of (i) the distributed nature of the data generated/collected by mobile devices, (ii) privacy concerns on sharing the local data with a central server, especially when the computational server is managed by a third party operator, and (iii) limited wireless resources (in terms of bandwidth and power). Therefore, privacy-preserving distributed AI techniques have become the cornerstone of recent advancements in AI applications over

wireless networks. In most distributed training algorithms, a set of devices upload their local updates (in terms of e.g., gradients in distributed stochastic gradient descent [5], or local models in federated learning (FL) [6]) via uplink (UL) channel to a master node (or a set of nodes) that maintains global parameters. Once the master node updates the global model, it shares them with the devices in a downlink (DL) channel.

Nevertheless, the UL/DL transmissions of AI gradients/models are prone to errors and delays by the wireless channel, impacting the learning performance in terms of convergence time [7]. There can be two remarks for distributed training on wireless systems. On the one hand, in addition to the number of iterations, the convergence time of the distributed training algorithm depends on the amount of time in which global model parameters are transmitted to the devices, trained locally, and transmitted back to the master node. On the other hand, the general perception is that increasing the AI model size improves the training accuracy [8], given enough data samples and a proper training approach that reduces over-fitting. However, using a larger AI model means longer communication and computation time, resulting in higher convergence time [7]. Higher AI communication overheads may also be detrimental for other communication services running in parallel to the AI. The tighter the requirements of the underlying service, the harder to design smooth coexistence.

Ultra-reliable low-latency communications (URLLC) is characterized by strict requirements in terms of latency, which could be as short as 500 μ s, and availability, which could be as high as 99.999999 [9]. Regarded as the most challenging use case in fifth generation of mobile communication systems (5G) and beyond 5G, this type of service is supposed to enable challenging applications (e.g., factory automation or autonomous intelligent transport systems [10]) that have not been feasible in preceding generations of wireless communications.

As distinct services, the performance of both URLLC and distributed AI over wireless networks have been widely investigated in the existing literature. However, the coexistence of URLLC, with its stringent requirements, and distributed AI workflow, with its unique traffic model and performance characteristics, have not yet been discussed in the literature. Such coexistence introduces new fundamental challenges as well as unique trade-offs between URLLC latency and availability on the one hand, and convergence time and accuracy

of distributed AI on the other hand. Notice that there are fundamental differences between AI service and other traditional communication traffic. In particular:

- Due to the statistical correlation of the data among different nodes, the missing gradients/models of some nodes can be approximated by the ones of other nodes, and we can run distributed learning workflow seamlessly.
- Due to the local smoothness of most objective functions used for the training, the training algorithm (and therefore the master node) may tolerate getting late updates from some devices or even use some outdated local gradients/models to update global parameters [11].

These are unique characteristics of distributed learning that distinguishes it from other traditional communication services.

In this paper, we address the following research questions:

- What are the trade-offs between URLLC availability and distributed AI convergence time and accuracy?
- How does the AI setting (e.g., model size, the number of participating AI devices, or the number of extra workers providing resilience against straggling) impact its own and the URLLC performance?

We address the above research questions with 3rd Generation Partnership Project (3GPP) compliant 5G-NR simulations using network and link level simulations. Within our simulations, we observe that the number of participating AI devices can have a significant impact on URLLC performance. Moreover, we show that introducing a soft synchronous protocol, in which the master node initiates the global model update upon receiving local updates from a portion of the participating devices, can help reduce the training delay in the order of seconds. Our results are also an important contribution to the ongoing standardization activities on 5G and beyond 5G to support distributed AI model distribution and transfer.

The rest of this paper is organized as follows. In Section II, we discuss related works and introduce URLLC and distributed AI key performance indicators (KPIs). We describe our link level and network level simulations in Section IV. Section V presents the main results and insights on the coexistence scenario. Section VI concludes the paper.

Notations: Normal font x or X , bold font \mathbf{x} or \mathbf{X} , and uppercase calligraphic font \mathcal{X} denote scalar, vector and set, respectively. We denote by $|\mathcal{X}|$ the cardinality of set \mathcal{X} , by $\mathbb{1}\{x\}$ the indicator function taking 1 only when condition x holds, and by $[N]$ set $\{1, 2, \dots, N\}$.

II. BACKGROUND AND SYSTEM MODEL

A. Distributed Learning

Consider the problem of minimizing a sum of functions $\{f_i : \mathbb{R}^d \mapsto \mathbb{R}\}_{i \in [N]}$, with corresponding gradients $\{\nabla f_i : \mathbb{R}^d \mapsto \mathbb{R}^d\}_{i \in [N]}$:

$$\mathbf{w}^* := \min_{\mathbf{w} \in \mathbb{R}^d} f(\mathbf{w}) = \min_{\mathbf{w} \in \mathbb{R}^d} \frac{1}{N} \sum_{i \in [N]} f_i(\mathbf{w}). \quad (1)$$

Such problems frequently arise in distributed learning where each f_i could represent a local model. In practice, to parallel

the computations or to preserve the privacy of local datasets, we use distributed algorithms to solve (1) [12]. That is, at iteration k , a subset of the workers compute and upload their gradients $\{\nabla f_i(\mathbf{w}_k)\}_i$ to a master node, which updates the model and broadcasts the updated model parameters \mathbf{w}_{k+1} to the workers. Federated learning is another popular method in which the workers will run one or several local training passes and upload their local models afterward. The master node will then take a global average over them. The communication overhead is almost the same as uploading gradients [3]. However, most of these uplink messages (gradients or local models) are redundant, carrying almost no additional information since they can be retrieved from their past communicated messages as well as messages of other devices [13]. Forcing some of them to remain silent would 1) reduce uplink interference to other users, 2) increase throughput, and 3) improve latency.

In conventional synchronous distributed training methods, the master node should wait to receive the local updates from all participating devices, leading to a considerable inoperative time in the master node waiting for stragglers. To tackle the straggler's problem, in n -synch approaches, the master node only waits for a subset of participating devices, say n out of all N devices, and updates the global model using their messages at every iteration [5]. Nevertheless, vanilla n -synch-based methods add extra load on the underlying communication system, as they will ask all the devices to upload their data, and the master node starts its update with the first n received data. Reference [14] proposed an algorithm to adjust n at every iteration. References [6], [13], [15] proposed various approaches to eliminate some unnecessary uploads. However, none of those works study or optimize the interplay between distributed learning and other parallel communication services.

B. System Model

We consider an industrial automation scenario where a set of $\mathcal{M} := [M]$ industrial devices in the factory hall execute different functions that enable automated production. The communication system should timely and reliably deliver (i) monitoring data to gNodeBs (gNBs) and (ii) computed or emergency control commands to the actuators. However, we consider application-layer performance for URLLC service, implying that consecutive failures that are shorter than survival time (T_{sv}) do not affect the end-to-end performance.

For simplicity, we assume that AI devices are distinct from industrial devices, and there exist a set of participating AI devices $\mathcal{U} := [N]$ serving a background AI task. Moreover, we assume that the AI master node requires to receive the relevant local information from n out of these N participating AI devices to update its global model. For simplicity, we define $\eta := \frac{n}{N}$. Therefore, we obtain fully synchronous and n -synch distributed training for $\eta=1$ and $\eta<1$, respectively.

To manage the coexistence of two services, where the priority of services are inherently different, 5G and beyond 5G envision two approaches. The first approach, employed in this paper, is to use the existing standardized protocols in 5G-NR for quality of service (QoS) handling. In this case,

each connected device is assigned with one or several QoS flows and data radio bearers, where the former is set in the core network, depending on the service QoS requirements. For example, in our scenario, the traffic from/to URLLC devices is set to have high priority QoS flow to ensure low latency, whilst the traffic from/to AI devices is set to have low priority QoS flow. Each (or several) of these QoS flows are then mapped to a data radio bearer in the radio access network. In gNB and devices, there is an associated radio link control (RLC) buffer to each data radio bearer, and in our case, with strict priority scheduling [16]. The second approach, as we foresee, is to have separate slices for URLLC and distributed AI, resulting in full resource separation (e.g., in terms of bandwidth).

To model a distributed learning task, we consider a network of N AI devices that cooperatively solve a distributed learning problem. Iteration k of an abstract distributed algorithm reads:

$$\mathbf{w}_{k+1} = A(\mathbf{c}_{i,k+1}, \mathbf{w}_k), \quad \text{for } \forall i \in \mathcal{U}_n \quad (2a)$$

$$\mathbf{c}_{i,k+1} = C_i(\mathbf{w}_{k+1}), \quad \text{for } \forall i \in \mathcal{U} \quad (2b)$$

where function A represents an algorithm update of the decision variable \mathbf{w}_k , function C_i picks out the relevant information, $\mathbf{c}_{i,k}$, that node i uploads to the server to run the algorithm. This general algorithmic framework covers many machine learning (ML) algorithms, including federated learning and distributed stochastic gradient descent, with or without data compression. For example, when C_i returns a stochastic gradient, say $\hat{\nabla} f_i(\mathbf{w}_{k+1})$, and $A = \mathbf{w}_k - \alpha \sum_i \hat{\nabla} f_i(\mathbf{w}_{k+1})/n$ for some positive step size α , we recover n -synchron and synchronous distributed stochastic gradient descent for $n(<N)$ and $n(=N)$. When C_i returns an updated local model parameters of AI device i and A takes an averaging step over a subset of $n(\leq N)$ AI devices, we recover FL (n -synchron or synchronous).

In the next section, we use these models to formulate performance metrics.

III. PERFORMANCE METRICS

A. URLLC: Application Layer Availability

The reliability of URLLC service is typically identified by application layer availability, where such KPI is measured at the application layer of the end device [9]. In terms of reliability, the main difference between the observed performance on the application layer with the observed performance on the network layer is driven by a system parameter called survival time, T_{sv} . Survival time is a duration of time for which the application layer can tolerate failures in the communication system without any performance degradation in availability [17]. Let us denote the communication system state variable by a Bernoulli state variable $X_i(t)$, where $X_i(t)$ for the i th URLLC device is zero if the last packet reception at network layer has failed, either because it could not be decoded at the lower layers or the packet has been received after its corresponding delay bound. Consequently, we define the per-

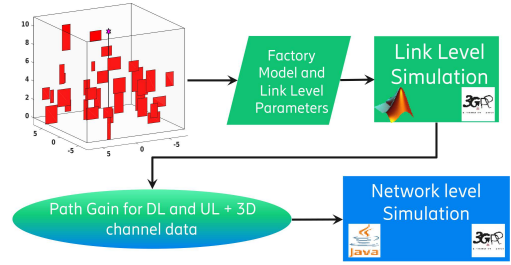


Fig. 1: The simulation setup.

device application layer state variable, $Y(t)$ as

$$Y_i(t) := \begin{cases} 0 & \text{if } \int_{\tau=t-T_{sv}}^t X_i(\tau) d\tau = 0, \\ 1 & \text{otherwise.} \end{cases} \quad (3)$$

Therefore, we can define the long-term availability of the i th industrial device as [2]

$$a_i := \lim_{T \rightarrow \infty} \Pr \{Y_i(t) = 1\} = \lim_{T \rightarrow \infty} \frac{1}{T} \int_{t=0}^T Y_i(t) dt. \quad (4)$$

The availability can be estimated over a short time using

$$\bar{a}_i := \frac{1}{T} \int_{t=0}^T Y_i(t) dt. \quad (5)$$

In URLLC applications, the requirement is often defined in the form of [18]

$$\Pr \{a_i \leq a_i^{\text{req}}\} \leq \gamma, \forall i \in \mathcal{M}, \quad (6)$$

where a_i^{req} is the availability requirement for URLLC device i , and γ is the sensitivity of the application to a_i^{req} .

B. Distributed AI: Training Delay

The convergence time of the distributed AI is bounded by the communication and processing latency [7]. Let us assume $\mathcal{U}_n \subseteq \mathcal{U}$ where $|\mathcal{U}_n| = n$. Based on the abstract distributed algorithm in Section II-B, the AI training delay in the master node for k th iteration, d_k^{AI} , can be derived as

$$d_k^{\text{AI}} = \min_{\forall \mathcal{U}_n \subseteq \mathcal{U}} \left[\max_{\forall i \in \mathcal{U}_n} \left(d_{i,k}^{\text{D}} + d_{i,k}^{\text{pr}} + d_{i,k}^{\text{U}} + d_k^{\text{pr}} \right) \right], \quad (7)$$

where $d_{i,k}^{\text{D}}$, $d_{i,k}^{\text{pr}}$, and $d_{i,k}^{\text{U}}$ are the latency of DL global model broadcasting, local training (represented in (2b)), and UL transmission of local gradients/models for k th iteration of i th device, respectively. It is worth noting that $d_{i,k}^{\text{D}}$ and $d_{i,k}^{\text{U}}$ include the transmission processing, payload transmission, and queuing delay, which is determined by the number of devices sharing the same time-frequency resources. Besides, d_k^{pr} is the k th iteration processing delay required to perform the global model update on the master node, represented in (2a). Thus, in equation (7), for each subset, the maximum aggregated communication and processing delay is calculated among devices. Then, among subsets, d_k^{AI} is determined by picking the subset with the lowest delay.

IV. SIMULATION METHODOLOGY

For simulating the URLLC and distributed AI coexistence deployment, we performed both link level and network level

simulations for a factory automation scenario (as shown in Fig. 1). More explicitly, we designed a 3D model of a small factory of size $15 \times 15 \times 11 \text{ m}^3$ with a gNB in the middle at the height of 10 m. We assumed that the gNB is configured with a 3-sector cell setting. In link level simulations, we modeled blockers with the width and height that are uniformly selected from the range of $[0.5, 2] \text{ m}$ and $[1, 3] \text{ m}$, respectively, and positioned them randomly inside the factory. We leveraged the blockage model B from [19] to determine the multipath attenuation caused by each of the blockers using a knife-edge diffraction method. The path gain matrix and 3D channel data for all possible devices' locations are then imported to a network level simulator in which we simulated physical (PHY), medium access control (MAC), and above layers in a multi-cell multi-user scenario.

The network level simulator is event-based, 3GPP compliant, and operates at orthogonal frequency-division multiplexing (OFDM) symbol resolution. We considered numerology one from [16], implying that each slot and symbol are 0.5 ms and $33.33 \mu\text{s}$ long, respectively. At each seed, the location of both URLLC and AI devices are selected randomly. To ensure seamless training of distributed AI until the end of a simulation, we considered RLC in acknowledged mode (AM) for distributed AI. Nevertheless, the RLC retransmissions are slow and unlikely to benefit URLLC packets with their tight delay bounds [16]. Accordingly, we configured the RLC in unacknowledged mode (UM) for URLLC flow. Besides, we assumed strict priority scheduling where URLLC flow has higher priority than AI flow, implying that AI packets can not be scheduled unless there is no URLLC packet on the queues.

Upon transmission, one or several packets are drawn from the head of the corresponding RLC buffer, depending on the selected modulation and coding scheme on lower layers. Alternatively, RLC could perform segmentation of packets into smaller segments to fit them into transport blocks via which the packets are transmitted. Upon reception, the received instantaneous signal to noise and interference ratio (SINR) of each transport block (which depends on the radio channel and the dynamic interference of other devices' transmissions) determines an error probability. Consequently, the receptive RLC entity reassembles successfully decoded segments and delivers them to the application layer. For availability calculation on the application layer, we considered a URLLC packet lost if it is not fully received before its corresponding delay bound, followed by applying T_{sv} as in (5) where T is the duration of one simulation. TABLE I presents the simulation parameters.

On the traffic modeling, we considered 10 URLLC devices. The URLLC traffic is represented by periodic UL and DL traffic, with delay bound of 6 ms and 2 ms as well as size of 64 bytes and 80 bytes , respectively, both with period 5 ms . Motivated by [20], we assumed that the shared deep neural network (DNN) architecture (i.e., used on the devices and the master node) follows MobileNets [8], a class of efficient DNN models based on a streamlined architecture for mobile and embedded vision applications. We considered x MobileNet-224 in [8], where $x \in \{0.25, 0.5, 0.75, 1\}$, implying

TABLE I: Simulation Parameters

Parameter	Value
Deployment	1 gNB, 3 cells
Duplex/Carrier frequency	FDD/2600 MHz
Blocker's density	0.15 blocker/m ²
gNB antenna height	10 m
Devices' height	1.5 m
Carrier frequency	2.6 GHz
Bandwidth	40 MHz
TTI length/Subcarrier spacing	0.5 ms/30 KHz
UL/DL transmit power	0.2 W/0.5 W
Max num of UL/DL URLLC Trans. (MAC)	3/2
Max num of UL/DL AI Trans. (MAC)	10/10
Max num of UL/DL AI Trans. (RLC)	8/8
UL/DL URLLC delay bound	6/2 ms
UL/DL URLLC Survival time (T_{sv})	5/5 ms
Simulation time	100 s

that the DNN model can have 0.5, 1.3, 2.6, or 4.2 million parameters, respectively. To model the distributed AI traffic, we assumed FL and 32 bits quantization for each model parameter, implying that each model (local or global) can be represented by a size of 2 MB, 5.2 MB, 10.4 MB 16.8 MB in the case of 0.25 MobileNet, 0.5 MobileNet, 0.75 MobileNet, and 1 MobileNet, respectively.

V. RESULTS AND DISCUSSION

In this section, we evaluate the performance of URLLC and distributed AI in our coexistence scenario. Besides evaluating the impact of N , we study n -synch on the coexistence scenario from two different perspectives:

- **Eval1:** We compare cases with the same N , while changing η from 0.4 to 1, to address the impact of tightening the requirements for a global update at the master node.
- **Eval2:** We compare cases with the same $n (= \eta \times N)$, implying that the global model is aggregated from the same number of local models. Here, we evaluate the impact of $N - n$ extra devices available to reduce sensitivity to straggling devices.

Besides, we use (N, η) after a specific Eval to refer to N and η in a specific evaluation. For example, Eval2(50, 0.6) refers to $N=50$ and $\eta=0.6$ for an Eval2 experiment.

Fig. 2 illustrates the impact of introducing distributed AI workflow on URLLC service performance. Fig. 2a and Fig. 2b assume 0.25 MobileNet and 1 MobileNet [8], respectively. These figures show the median and the 1st percentile availability of the URLLC devices, while having different number of AI devices, N , and for different reception requirement, η . The dotted horizontal line represents α_i^{req} in (6), where we assumed it is identical for all URLLC devices (i.e., $\alpha_i^{\text{req}} = \alpha^{\text{req}} = 0.95$ for $\forall i \in \mathcal{M}$). We assumed $\gamma=0.01$, hence, if the first percentile availability is higher than the dotted line, the availability requirement in (6) is fulfilled. There is no notable difference observed between 0.25 MobileNet of Fig. 2a and 1 MobileNet of Fig. 2b. As both figures confirm, introducing the AI traffic causes a minimum of 0.037 decrease in the 1st percentile URLLC availability. This is shocking as our deployment supports two nines availability in the URLLC-only scenario, whilst it barely fulfills availability of 0.96 in the coexistence scenario. This significant availability reduction highlights the

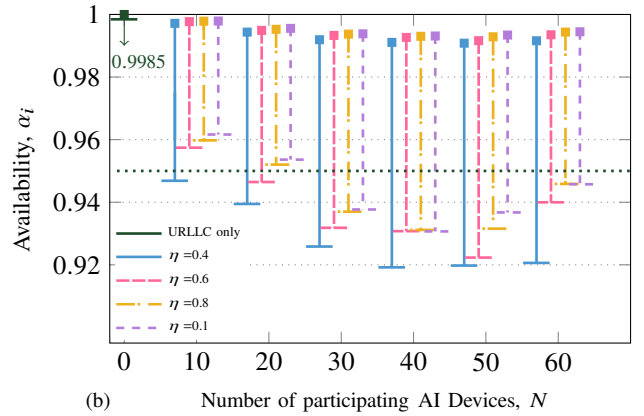
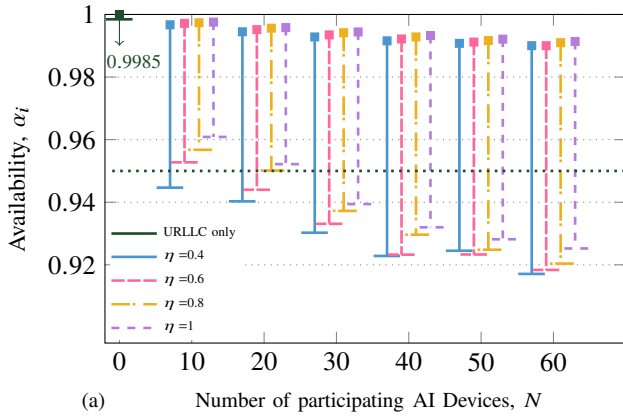


Fig. 2: Median (square) and 1st percentile (line) availability of URLLC, when training (a) 0.25 MobileNet, and (b) 1 MobileNet, both with 32 bits quantization.

importance of intelligent user selection or slicing approaches to control the effect of AI traffic-induced interference on URLLC service. Moreover, Fig. 2 shows that the availability of URLLC devices declines as we increase the number of AI participants. Generally, a higher number of distributed AI participants increases the interference, resulting in higher (i) packet error ratio and (ii) URLLC packet delays (since the scheduler requires to select lower modulation and coding scheme indices to cope with the higher interference). Consequently, the URLLC service does not meet its availability requirement, i.e., 0.95, when $N \geq 30$.

Fig. 3 depicts the distribution of per-iteration delay of distributed AI, d_k^{AI} formulated in (7), for different N and η with 0.25 MobileNet (Fig. 3a), 0.5 MobileNet (Fig. 3b), 0.75 MobileNet (Fig. 3c), and 1 MobileNet (Fig. 3d). Each box represents the minimum, 25th percentile, median, 75th percentile and maximum observed training delay (refer to the example box in Fig. 3a). In general, the distributed AI training delay rises with the number of distributed AI participants.

On Eval1, Fig. 3 shows that higher η results in higher training delay. As η grows, the master node should wait for a larger portion of participating devices in which it is more likely to include stragglers in poor channel condition, thus leading to higher training delay. This higher training delay could explain the improvement in availability in Fig. 2 for Eval1 case. For example, Fig. 3d shows that the median training delay for Eval1(60,1) increases 22% from Eval1(60,0.4) to 55.6 s. Hence, it is much more likely for AI devices in Eval1(60,1) to wait for the global model from master node, while the master node itself is waiting to receive the local models from stragglers. Such excessive pause in training leads to 2.7% improvement in 1st percentile availability for Eval1(60,1) compared to Eval1(60,0.4) in Fig. 3d. However, from convergence perspective, for a given \mathcal{U} , increasing η results in a lower variance for the gradient noise, potentially decreasing the number of iterations required to converge [12].

For Eval2, our results in Fig. 2 and Fig. 3 demonstrate that using extra devices to leverage diversity, and thus alleviating the stragglers' problem, can lead to contradicting outcome (i.e., it could reduce the 1st percentile availability by several percents and increase the training delay by tens of seconds).

For example, in Fig. 2b, the Eval2(50,0.6)'s 1st percentile availability is down to 0.922 from 0.937 in Eval2(30,1). Not to mention Fig. 3d, where the median of the training delay for Eval2(50,0.6) is 43.5, 1.5x the median training delay for Eval2(30,1). It seems that (i) high load, which is due to the transmission of large local and global models, and (ii) limited bandwidth on our system contributed to this contradictory outcome, thus overweighting the diversity gain.

The results in [8] on the ImageNet dataset (a substantial visual database intended for use in the research on visual object recognition) show that 0.25 MobileNet, 0.5 MobileNet, 0.75 MobileNet, and 1 MobileNet could achieve an accuracy of 50.6%, 63.7%, 68.4%, and 70.6%, respectively. From Fig. 3, the higher accuracy of bigger models comes at the price of a higher distributed AI training delay per global update iteration. This higher per-iteration complexity, together with the need for having more iterations for bigger models to converge result in a much higher convergence time. Furthermore, on the one hand, the accuracy of distributed AI rises with the number of participating AI devices. However, as the number of participating AI devices continues to grow, the rate of such increase decelerates [7]. On the other hand, our results in Fig. 2 and Fig. 3 reveal that the number of participating AI devices (N) heavily affects α_i and d_k^{AI} . These trade-offs highlight the significance of efficient user selection in implementing distributed AI techniques on future cellular networks.

VI. CONCLUSIONS

In this paper, we studied the trade-offs between the availability of URLLC service and the convergence time of distributed training. We leveraged the already existing 5G-NR QoS handling to separate the traffic of the two services. Using our near-product 3GPP-compliant simulations, we showed that the introduction of AI traffic has a considerable side effect on URLLC availability, which declines with the number of participating AI devices. Although an increase in the number of AI devices can improve the training accuracy of the distributed AI, we showed that the cost could be an intolerable increase in training delay, thanks to the 5G-NR scheduler.

As for future directions, we note that user-selection algorithms that jointly consider distributed AI's performance

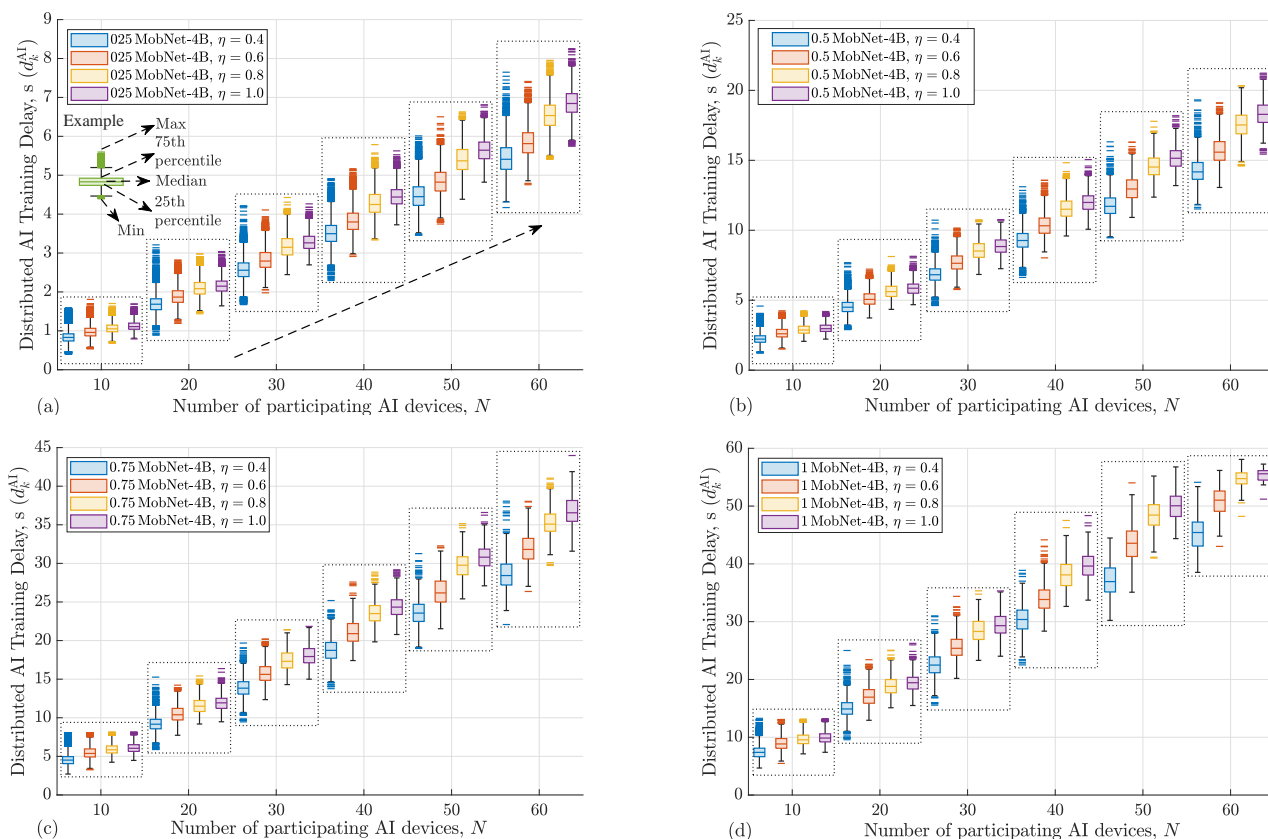


Fig. 3: The distribution of the distributed AI training delay, d_k^{AI} , for different η and N . Each box plot represents the minimum, 25th percentile, median, 75th percentile, and maximum of the observed training delay samples per iteration (as shown via the example in (a) with green box) for a specific η and N .

and the coexisting URLLC service are of crucial importance. Besides, new dynamic slicing approaches that optimize bandwidth allocation for AI slice and URLLC slice can improve the coexistence performance.

ACKNOWLEDGMENT

The authors would like to sincerely thank Abdulrahman Alabbasi and Jonas Kronander for their insightful comments.

REFERENCES

- [1] Y. Shi, K. Yang, T. Jiang *et al.*, “Communication-efficient edge AI: Algorithms and systems,” *IEEE Commun. Surveys Tuts.*, vol. 22, no. 4, pp. 2167–2191, 2020.
- [2] M. Ganjalizadeh, A. Alabbasi, A. Azari *et al.*, “An RL-based joint diversity and power control optimization for reliable factory automation,” in *IEEE Global Commun. Conf. (GLOBECOM)*, 2021.
- [3] T. Li, A. K. Sahu, A. Talwalkar, and V. Smith, “Federated learning: Challenges, methods, and future directions,” *IEEE Signal Process. Mag.*, vol. 37, no. 3, pp. 50–60, 2020.
- [4] A. Alabbasi, M. Ganjalizadeh, K. Vandikas, and M. Petrova, “On cascaded federated learning for multi-tier predictive models,” in *IEEE Int. Conf. on Commun. Workshops (ICC Workshops)*, 2021.
- [5] S. Dutta, G. Joshi, S. Ghosh *et al.*, “Slow and stale gradients can win the race: Error-runtime trade-offs in distributed SGD,” in *Proc. 21st Int. Conf. Artif. Intell. Stat. (AISTATS)*, 2018.
- [6] B. McMahan, E. Moore, D. Ramage *et al.*, “Communication-efficient learning of deep networks from decentralized data,” in *Proc. 20th Int. Conf. Artif. Intell. Stat. (AISTATS)*, 2017.
- [7] M. Chen, H. V. Poor, W. Saad, and S. Cui, “Convergence time optimization for federated learning over wireless networks,” *IEEE Trans. Wireless Commun.*, vol. 20, no. 4, pp. 2457–2471, 2021.
- [8] A. G. Howard, M. Zhu, B. Chen *et al.*, “MobileNets: Efficient convolutional neural networks for mobile vision applications,” 2017, *arXiv:1704.04861* [cs.CV].
- [9] *Service requirements for cyber-physical control applications in vertical domains*, 3GPP, Technical Specification (TS) 22.104 v18.0.0, 2021.
- [10] J. Sachs, G. Wikstrom, T. Dudda *et al.*, “5G radio network design for ultra-reliable low-latency communication,” *IEEE Netw.*, vol. 32, no. 2, pp. 24–31, 2018.
- [11] A. Agarwal and J. C. Duchi, “Distributed delayed stochastic optimization,” *Adv. Neural Inf. Process. Syst.*, vol. 24, 2011.
- [12] L. Bottou, F. Curtis, and J. Nocedal, “Optimization methods for large-scale machine learning,” *SIAM Review*, vol. 60, no. 2, pp. 223–311, 2018.
- [13] H. S. Ghadikolaei, S. Stich, and M. Jaggi, “LENA: Communication-efficient distributed learning with self-triggered gradient uploads,” in *Proc. 24th Int. Conf. Artif. Intell. Stat. (AISTATS)*, 2021.
- [14] S. Ji, W. Jiang, A. Walid, and X. Li, “Dynamic sampling and selective masking for communication-efficient federated learning,” *IEEE Intell. Syst.*, early access, 2021.
- [15] T. Chen, G. Giannakis, T. Sun, and W. Yin, “LAG: Lazily aggregated gradient for communication-efficient distributed learning,” in *Adv. Neural Inf. Process. Syst.*, 2018.
- [16] E. Dahlman, S. Parkvall, and J. Skold, *5G NR: The next generation wireless access technology*. Academic Press, 2018.
- [17] M. Ganjalizadeh, A. Alabbasi, J. Sachs, and M. Petrova, “Translating cyber-physical control application requirements to network level parameters,” in *IEEE 31st Int. Symp. Pers. Indoor Mob. Radio Commun. (PIMRC)*, 2020.
- [18] P. Popovski, Č. Stefanović, J. J. Nielsen *et al.*, “Wireless access in ultra-reliable low-latency communication (URLLC),” *IEEE Trans. Commun.*, vol. 67, no. 8, pp. 5783–5801, 2019.
- [19] *Study on channel model for frequencies from 0.5 to 100 GHz*, 3GPP, Technical Report (TR) 38.901 v17.0.0, 2022.
- [20] *5G System (5GS): Study on traffic characteristics and performance requirements for AI/ML model transfer*, 3GPP, Technical Report (TR) 22.874 v18.2.0, 2021.